JACS
JOURNAL OF THE AMERICAN CHEMICAL SOCIETY
Communication
pubs.acs.org/JACS

Plating a Dendrite-Free Lithium Anode with a Polymer/Ceramic/Polymer Sandwich Electrolyte

Weidong Zhou,[†] Shaofei Wang,[†] Yutao Li,[†] Sen Xin, Arumugam Manthiram, and John B. Goodenough*

Materials Science and Engineering Program & Texas Materials Institute, The University of Texas at Austin, Austin, Texas 78712, United States

Supporting Information

ABSTRACT: A cross-linked polymer containing pendant molecules attached to the polymer framework is shown to form flexible and low-cost membranes, to be a solid Li^+ electrolyte up to 270 °C, much higher than those based on poly(ethylene oxide), to be wetted by a metallic lithium anode, and to be not decomposed by the metallic anode if the anions of the salt are blocked by a ceramic electrolyte in a polymer/ceramic membrane/polymer sandwich electrolyte (PCPSE). In this sandwich architecture, the double-layer electric field at the Li/polymer interface is reduced due to the blocked salt anion transfer. The polymer layer adheres/wets the lithium metal surface and makes the Li-ion flux at the interface more homogeneous. This structure integrates the advantages of the ceramic and polymer. With the PCPSE, all-solid-state Li/$LiFePO_4$ cells showed a notably high Coulombic efficiency of 99.8–100% over 640 cycles.

Today's lithium-ion batteries use a flammable organic liquid electrolyte that is reducible at the surface of an anode until a Li^+-permeated solid electrolyte interphase (SEI) passivating layer is formed; this process leads to an irreversible loss of lithium from the cathode and lowers Coulombic efficiency.[1−5] In addition, lithium dendrites form during plating of metallic lithium on charge and can grow across a thin separator to short-circuit a cell with incendiary consequences. The assembly of a discharged cell with a carbon anode has permitted rechargeable lithium-ion batteries for hand-held devices, but the carbon anode has a low anode capacity and limits the rate of recharge of a cell.[6,7] Safety concerns and the requirement of higher energy density have stimulated a search for a durable all-solid-state battery with an inorganic or dry polymer electrolyte that is more stable toward lithium metal and can suppress the growth of lithium dendrites.[8−12]

In conformity with this strategy, various lithium-conducting inorganic and polymeric electrolytes have been explored.[8−12] However, neither inorganic nor polymeric electrolytes have yet been widely applied in commercial batteries due to their own drawbacks. Although Li-conductive ceramics combine a strong mechanical stiffness and a high Li^+ transfer number,[8,9] a relatively large solid–solid interfacial resistance for Li^+ transport has made it difficult to integrate a ceramic electrolyte directly into solid-state cells. Moreover, the anode–dendrite formation and growth in the grain boundaries of inorganic electrolyte membranes is even faster than in the traditional liquid electrolytes.[13,14]

Polymeric electrolytes based on poly(ethylene oxide) (PEO) have been the most extensively studied polymer systems.[15] However, the PEO only shows good Li^+ conductivity at temperatures higher than its melting point (65 ± 2 °C), which means the PEO electrolyte is a gel electrolyte rather than a solid-sate electrolyte. The PEO gel can gradually diffuse across the porous SEI layer and leads to an endless loss of lithium from the cathode. Another intrinsic obstacle to the application of PEO-based electrolytes in real batteries is a relatively low ionic transfer number (t_{Li^+}), generally around 0.2–0.5.[16−19] During charge, this low Li^+ transference number results in a rapid anion depletion to produce a large electric field across the Li/polymer interface, which leads to enhanced electrodeposition on the Li metal surface and accelerates the decomposition of the electrolyte and dendrite nucleation.[20−22]

Given the advantages and disadvantages of the inorganic and polymeric electrolytes discussed above, a combination of polymer/ceramic/polymer sandwich electrolyte (PCPSE) may integrate the benefits from different layers and address the problems of each. In the architecture of PCPSE, introduction of the ceramic layer blocks anion transport, which reduces the double-layer electric field at the Li/polymer interface and lowers the chemical/electrochemical decomposition of the polymer electrolyte to improve the Coulombic efficiency of a battery. On the other hand, a polymer electrolyte layer that is between the anode and a ceramic electrolyte can suppress dendrite nucleation due to the uniform Li^+ flux on the polymer/lithium interface and better wetting ability toward lithium metal and protects the ceramic layer from contacting the lithium metal. Although the PCPSE increases the resistance compared to an individual polymer electrolyte, the improved efficiency and good dendrite suppression capability make it more feasible in a solid-state battery.[23]

Here, we first synthesized a cross-linked Li^+ polymer conductor, which is solid at 270 °C, allowing the construction of lithium solid-state batteries. Combined with a ceramic membrane, a PCPSE (Figure 1a) was then constructed for an all-solid-state battery, and an all-solid-state $LiFePO_4$/Li cell delivered superior long-term electrochemical stability and a notably high Coulombic efficiency of 99.8–100%.

As shown in Figure 1b and Figure S1 of the Supporting Information, the cross-linked poly(ethylene glycol) methyl ether acrylate (CPMEA) established a three-dimensional network containing a polyacrylate main chain and oligoethylene oxide

Received: May 24, 2016
Published: July 21, 2016

DOI: 10.1021/jacs.6b05341
J. Am. Chem. Soc. 2016, 138, 9385–9388

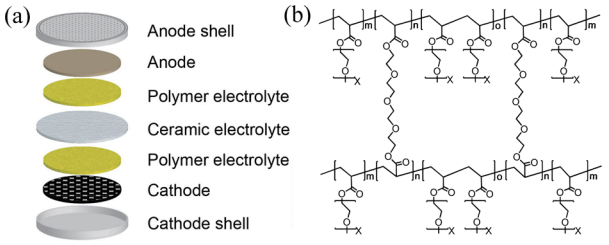

Figure 1. (a) Illustration of all-solid-state battery design with the PCPSE electrolyte. (b) Structure of polymer CPMEA.

pendants terminated by $-OCH_3$ units.[24] In this architecture, the electrochemically inert polyacrylate provides a stable framework and the oligoethylene oxide pendants attached to the framework swing freely, facilitating the ionic transfer of Li^+. Thermogravimetric analysis showed that the CPMEA did not exhibit an obvious weight loss until 270 °C, and the differential scanning calorimetry curve did not give an obvious endothermal melting process until 270 °C (Figure S2), indicating that the CPMEA-based membranes should have sufficient thermal stability to remain solid in a lithium metal battery. The polymer−electrolyte membranes were prepared by evaporation of a solution of polymer with lithium bistrifluoromethanesulfonylimide (LiTFSI) as a lithium salt; the thickness of membranes was controlled at 100 μm by adjusting the weight of the mixture in a mold (Figure S3).[25−28]

A typical 2032 coin cell of Li/CPMEA/stainless steel(Fe) was tested to examine the electrochemical stability window of the polymer electrolyte. The positive scans of the cyclic voltammetry (CV) curves in Figure 2a show that the electrolyte experiences a

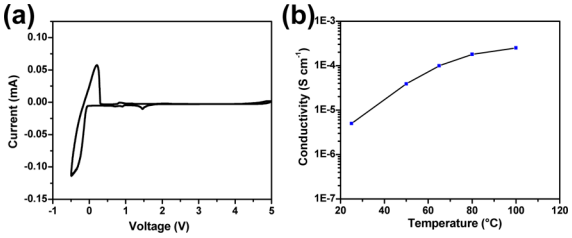

Figure 2. (a) CV curve of the Li/CPMEA−LiTFSI/Fe at 65 °C with a scan rate of 0.2 mV s^{-1}. (b) Ionic conductivity of a CPMEA−LiTFSI membrane versus temperature.

slight oxidation above 4.8 V, which indicates the electrolyte membrane could be stable at 4.8 V. On the negative scan, the CPMEA electrolytes experienced a symmetric lithium plating−stripping curve at −0.5 to +0.5 V. The small peaks located between 1 and 2 V in the CV curves can be attributed to the redox behaviors of the catalyst added during the preparation process. In order to make an accurate evaluation of electrochemical stability of the polymer at high voltage, the impedance of the polymer electrolyte was recorded after applying a continuous DC bias voltage for a long period (Figure S4). The impedance of Li/CPMEA/Fe only experienced a slight change after being subjected to 4.5 V vs Li/Li^+ for 300 h; the total impedance and interfacial resistance of the PEO electrolyte showed a huge continuous increase when an applied bias voltage was extende at 4.2 V for only 50 h, indicating the much improved electrochemical stability of the CPMEA network compared with that of the PEO electrolyte. Figure 2b illustrates the variation of ionic conductivity of the CPMEA−LiTFSI membranes at different temperatures. The conductivity shows an obvious increase with increasing temperature due to the gradual softening process of the polymer and the increasing movement of the pendant oligoethylene oxide group in the cross-linked polymer network. It can be seen that the ionic conductivity is around 1×10^{-4} S cm^{-1} at 65 °C, and the ionic conductivity further increases to 2×10^{-4} S cm^{-1} at 100 °C. To keep the mechanical strength of the polymer membrane, a measurement temperature of 65 °C was adopted in this study.

To test the PCPSE concept, a ceramic membrane of NASICON $Li_{1.3}Al_{0.3}Ti_{1.7}(PO_4)_3$ (LATP) was employed because the LATP has advantages over other inorganic materials in terms of the high lithium-ion conductivity and chemical stability in air.[29] The ionic conductivity of a CPMEA−LATP sandwich electrolyte was evaluated in a Li/Fe cell. As presented in Figure 3a, compared with the impedance spectrum of Li/CPMEA/Fe,

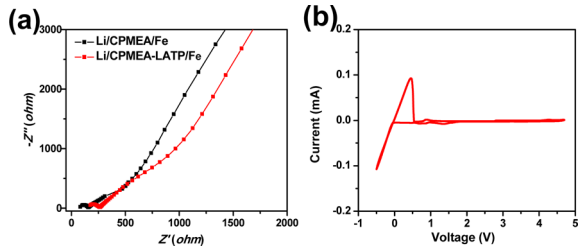

Figure 3. (a) Impedance spectra of CPMEA and CPMEA−LATP electrolyte in Li/Fe cells. (b) CV curve of Li/CPMEA−LATP/Fe at a voltage window of −0.5 to +4.75 V.

the resistance of Li/CPMEA−LATP/Fe is higher by 350 ohm, which can be attributed to the internal resistance of LATP and an interfacial impedance across CPMEA/LATP interfaces. The impedance data of the LATP membrane in Li/Fe cells are not given here because the LATP is reduced by lithium metal. The electrochemical working window of the CPMEA−LATP electrolyte was determined by CV scans in the Li/Fe cells, as shown in Figure 3b. The cell experienced only one symmetric plating−stripping curve at −0.5 to +0.5 V, and no obvious redox signal was observed until 4.75 V, indicating good electrochemical stability of the CPMEA−LATP at this voltage window.

Since $LiFePO_4$ has been shown to be a stable cathode, the CPMEA and CPMEA−LATP-based PCPSE electrolyte membranes were then tested in $LiFePO_4$/Li all-solid-state cells. The $LiFePO_4$ cathode membranes were prepared with the CPMEA as a polymer binder/ion conductor and carbon black as the electron conductor in a loading of 5 mg cm^{-2}, which is much higher than that generally used in thin-film electrodes for all-solid-state cells with ceramic electrolytes.[30] Figure 4a,b shows the charge/discharge voltage profiles of the $LiFePO_4$ cell at 0.2 and 0.5C with the CPMEA and PCPSE at 65 °C, respectively. The discharge capacities around 130 mAh g^{-1} at 0.2C (0.17 mA cm^{-2}) and 120 mAh g^{-1} at 0.5C (0.43 mA cm^{-2}) could be obtained for both electrolytes. These highly reproducible and well-defined plateaus of the characteristic $LiFePO_4$ electrodes verify that the PCPSE can function effectively as a solid electrolyte in a lithium battery. It can be seen that the charge/discharge plateau with the PCPSE electrolyte is flatter than that with only CPMEA as the electrolyte, and the Coulombic efficiency of the PCPSE electrolyte is obviously higher, although the cell polarization is slightly increased from CPMEA (0.15 V) to PCPSE (0.22 V) at 0.5C rate due to a higher impedance. Figure 4c shows a cycling performance of $Li/LiFePO_4$ cells with CPMEA and PCPSE at different C rates. At an initial 100 cycles, the capacities of Li/

DOI: 10.1021/jacs.6b05341
J. Am. Chem. Soc. 2016, 138, 9385−9388

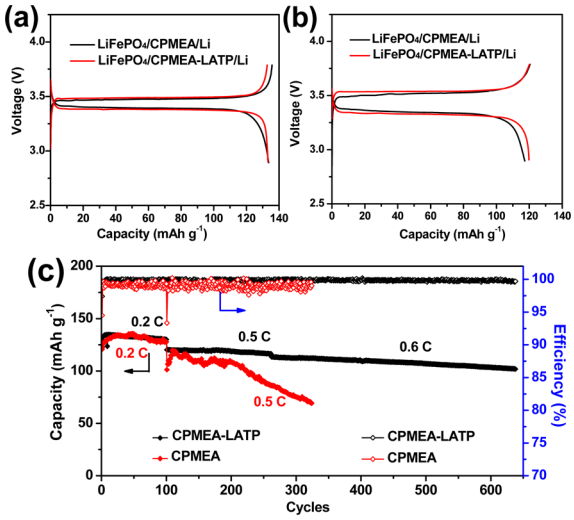

Figure 4. Charge and discharge voltage profiles of Li/$LiFePO_4$ cells with CPMEA and CPMEA−LATP-based PCPSE at 0.2C (a) and 0.5C (b). (c) Cycling and C rate performance of the Li/$LiFePO_4$ cells with CPMEA and CPMEA−LATP-based PCPSE.

$LiFePO_4$ cells with both electrolytes are pretty similar, but after 200 cycles, the capacity of Li/$LiFePO_4$ using CPMEA exhibited a rapid fading to 70 mAh g^{-1} after 325 cycles. In contrast, the capacity retention of Li/$LiFePO_4$ using PCPSE was still around 102 mAh g^{-1} at 0.6C (0.51 mA cm^{-2}) after 640 cycles, demonstrating more stable electrochemical behavior with the PCPSE. At a higher current of 1.0 mA cm^{-2} (around 1.2C), the Li/$LiFPO_4$ cell using PCPSE delivered a capacity of around 105 mAh g^{-1} (Figure S5). The Coulombic efficiency was kept at 99.9 ± 0.1% for a Li/$LiFPO_4$ cell using PCPSE after the initial 1−3 formation cycles and remained highly stable throughout cycling from 0.2 to 0.6C (even approaching 100% in many cycles). The Coulombic efficiency of a Li/$LiFPO_4$ cell using CPMEA electrolyte is around 99 ± 0.3% at 0.2C, which exhibits a larger fluctuation at 0.5C to 99 ± 1% during this cycling, similar to the Li/$LiFPO_4$ cell using widely reported PEO electrolyte (97−99%).[27,28] The impedance of the Li/$LiFePO_4$ cell with the individual CPMEA electrolyte after 325 cycles shows a significant increase, while the cell with PCPSE experienced a much lower impedance increase after 640 cycles and the charge−discharge profile is obviously flatter (Figures S6 and S7), indicating that the polymer electrolyte layer is electrochemically stabilized in the PCPSE during long cycling.

Compared with the individual polymer electrolyte, the improved cycling performance and efficiency of the PCPSE indicate better electrochemical stability and higher lithium plating/stripping efficiency across the polymer/lithium interface. More importantly, this long cycling stability also illustrates good dendrite growth suppression of PCPSE during the long-term Li plating/stripping process since the LATP would have been irreversibly reduced and short-circuited if a dendrite had penetrated across the polymer layer. The SEM images of lithium metal after cycling 640 cycles in a Li/CPMEA−LATP/Li$FePO_4$ cell does not show any obvious dendrite formation, although the lithium surface showed some cracks during the lithium plating/stripping process due to the volume expansion (Figure S8).

Generally, the lower Coulombic efficiency (i.e., the lithium loss) can be attributed to a decomposition of the polymer electrolyte by an alkali metal anode under an electric field. An illustration of the electric potential profile across the phase boundaries is given in Figure 5.[27,28,31] Within the contact region between two conducting phases, charge carriers in both phases

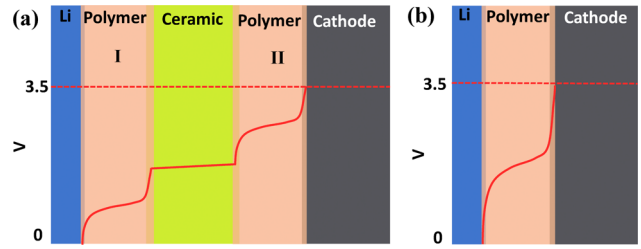

Figure 5. Illustration of the electric potential profile across the sandwich electrolyte (a) and individual polymer electrolyte (b) in the charge process of a Li/$LiFePO_4$ cell.

redistribute and create an electric double layer at the interface, forming a membrane potential difference at the interfaces. Due to a block of the anion of the polymer salt by the ceramic electrolyte layer, the t_{Li^+} is increased and the trapped positive charge at the anode/polymer interface is reduced (Figure 5a and Table S1), which reduces the magnitude of the electric field across the interface and facilitates stabilization of the polymer electrolyte. On the other hand, when the salt anion is not blocked in the absence of a ceramic layer (Figure 5b), a stronger interface electric field lowers the lowest unoccupied molecular orbital energy of the interface polymer relative to the anode Fermi energy to induce an electron transfer for an interfacial chemical reaction.[32,33]

On the other hand, wetting of the polymer surface by the lithium anode may not only reduce the Li^+ transfer resistance but also give a uniform Li^+ flux across the interface and thus suppress the dendrite formation. Without the polymer layer, the surface of a ceramic pellet cannot sufficiently contact the lithium and so cannot be uniformly wetted by the metallic lithium, even when chemically stable ceramic electrolytes were employed such as the garnet $Li_7La_3Zr_2O_{12}$ (LLZO). With an individual LLZO membrane, during the charge process, the Li^+ ions from the ceramic are plated preferentially on the ceramic grain boundaries where the Li-ion flux is locally enhanced under an electric field. The Li/$LiFePO_4$ cell and Li/Li symmetric cell using LLZO as an electrolyte without a polymer interlayer (Figure 6a and Figures

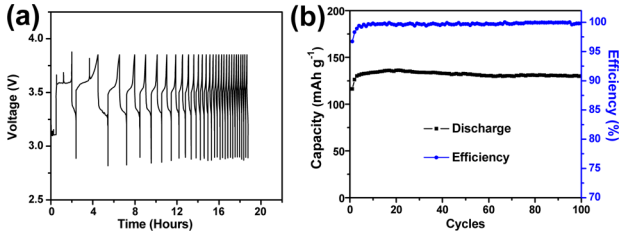

Figure 6. Charge and discharge voltage profiles of Li/LLZO/$LiFePO_4$ (a) and cycling performance of Li/$LiFePO_4$ with LLZO containing PCPSE at 65 °C and 0.2C.

S9 and S10) short-circuited in only 20 h, similar to previous studies.[13,14] With the polymer interlayer, homogeneous interfaces of ceramic membrane/polymer/lithium were constructed, where a more uniform Li-ion flux at the interface and better wetting and/or adhesion of the Li surface by the polymer were achieved. However, without the ceramic electrolyte to block the polymer salt anion from vacating the anode/polymer interface, an electric double-layer field becomes strong enough

DOI: 10.1021/jacs.6b05341
J. Am. Chem. Soc. 2016, 138, 9385−9388

to allow tunneling of electrons from the lithium anode to the polymer across a thin interfacial layer to react with the polymer and affect the long-term cycling performance.[34−36] Therefore, the sandwich structure integrates the benefits from different layers and delivers cells with high Coulombic efficiency and better suppression of dendrite formation. The Li/$LiFePO_4$ cell with the LLZO containing PCPSE delivers a stable capacity of 130 mAh g^{-1} after 100 cycles with an efficiency of 99.7−100%, indicating the superior stability and universal improvement of efficiency for the PCPSE-based solid electrolytes (Figure 6b).

In conclusion, we have demonstrated that a PCPSE having a cross-linked Li^+ polymer electrolyte and a ceramic membrane sandwiched within the polymer electrolyte can be used in an all-solid-state lithium battery. Moreover, blocking by the ceramic membrane of the polymer salt anion from vacating the lithium/polymer interface stabilizes the interface against degradation by electron transfer across it to provide a long cycle life cell with a metallic lithium anode. This observation shows that it is possible for a lithium anode to contact a polymer electrolyte if the polymer salt anion is immobilized.

■ ASSOCIATED CONTENT

Supporting Information

The Supporting Information is available free of charge on the ACS Publications website at DOI: 10.1021/jacs.6b05341.

Experimental procedures, characterizations, and electrochemical data (PDF)

■ AUTHOR INFORMATION

Corresponding Author

*jgoodenough@mail.utexas.edu

Author Contributions

†W.Z., S.W., and Y.L. contributed equally.

Notes

The authors declare no competing financial interest.

■ ACKNOWLEDGMENTS

The polymer development work was supported by the National Science Foundation Grant No. CBET-1438007, and the solid electrolyte development work was supported by the U.S. Department of Energy, Office of Basic Energy Sciences, Division of Materials Sciences and Engineering, under Award No. DE-SC0005397.

■ REFERENCES

(1) Tarascon, J. M.; Armand, M. *Nature* **2001**, *414*, 359−367.
(2) Armand, M.; Tarascon, J. M. *Nature* **2008**, *451*, 652−657.
(3) Whittingham, M. S. *Chem. Rev.* **2004**, *104*, 4271−4301.
(4) Thackeray, M. M.; Wolverton, C.; Isaacs, E. D. *Energy Environ. Sci.* **2012**, *5*, 7854−7863.
(5) Liu, C.; Li, F.; Ma, L.-P.; Cheng, H.-M. *Adv. Mater.* **2010**, *22*, E28−E62.
(6) Goodenough, J. B.; Kim, Y. *Chem. Mater.* **2010**, *22*, 587−603.
(7) Xu, K. *Chem. Rev.* **2014**, *114*, 11503−11618.
(8) Cao, C.; Li, Z.-B.; Wang, X.-L.; Zhao, X.-B.; Han, W.-Q. *Front. Energy Res.* **2014**, *2*, 25.
(9) Quartarone, E.; Mustarelli, P. *Chem. Soc. Rev.* **2011**, *40*, 2525−2540.
(10) Manuel Stephan, A.; Nahm, K. S. *Polymer* **2006**, *47*, 5952−5964.
(11) Song, J. Y.; Wang, Y. Y.; Wan, C. C. *J. Power Sources* **1999**, *77*, 183−197.
(12) Dias, F. B.; Plomp, L.; Veldhuis, J. B. J. *J. Power Sources* **2000**, *88*, 169−191.
(13) Sudo, R.; Nakata, Y.; Ishiguro, K.; Matsui, M.; Hirano, A.; Takeda, Y.; Yamamoto, O.; Imanishi, N. *Solid State Ionics* **2014**, *262*, 151−154.
(14) Ren, Y.; Shen, Y.; Lin, Y.; Nan, C.-W. *Electrochem. Commun.* **2015**, *57*, 27−30.
(15) Croce, F.; Appetecchi, G. B.; Persi, L.; Scrosati, B. *Nature* **1998**, *394*, 456−458.
(16) Capuano, F.; Croce, F.; Scrosati, B. *J. Electrochem. Soc.* **1991**, *138*, 1918−1922.
(17) Appetecchi, G. B.; Zane, D.; Scrosati, B. *J. Electrochem. Soc.* **2004**, *151*, A1369−A1374.
(18) Evans, J.; Vincent, C. A.; Bruce, P. G. *Polymer* **1987**, *28*, 2324−2328.
(19) Ghosh, A.; Wang, C.; Kofinas, P. *J. Electrochem. Soc.* **2010**, *157*, A846−A849.
(20) Chazalviel, J.-N. *Phys. Rev. A: At., Mol., Opt. Phys.* **1990**, *42*, 7355−7367.
(21) Rosso, M.; Gobron, T.; Brissot, C.; Chazalviel, J. N.; Lascaud, S. *J. Power Sources* **2001**, *97−98*, 804−806.
(22) Brissot, C.; Rosso, M.; Chazalviel, J.-N.; Lascaud, S. *J. Power Sources* **1999**, *81−82*, 925−929.
(23) Doyle, M.; Fuller, T. F.; Newman, J. *Electrochim. Acta* **1994**, *39*, 2073−2081.
(24) Sun, X. G.; Kerr, J. B.; Reeder, C. L.; Liu, G.; Han, Y. B. *Macromolecules* **2004**, *37*, 5133−5135.
(25) Tu, Z.; Kambe, Y.; Lu, Y.; Archer, L. A. *Adv. Energy Mater.* **2014**, *4*, 1300654.
(26) Khurana, R.; Schaefer, J. L.; Archer, L. A.; Coates, G. W. *J. Am. Chem. Soc.* **2014**, *136*, 7395−7402.
(27) Yuan, C.; Li, J.; Han, P.; Lai, Y.; Zhang, Z.; Liu, J. *J. Power Sources* **2013**, *240*, 653−658l.
(28) Gerbaldi, C.; Nair, J. R.; Kulandainathan, M. A.; Kumar, R. S.; Ferrara, C.; Mustarelli, P.; Stephan, A. M. *J. Mater. Chem. A* **2014**, *2*, 9948−9954.
(29) Suzuki, T.; Yoshida, K.; Uematsu, K.; Kodama, T.; Toda, K.; Ye, Z.-G.; Ohashi, M.; Sato, M. *Solid State Ionics* **1998**, *113−115*, 89−96.
(30) Li, J.; Ma, C.; Chi, M.; Liang, C.; Dudney, N. J. *Adv. Energy Mater.* **2015**, *5*, 1401408.
(31) Busche, M. R.; Drossel, T.; Leichtweiss, T.; Weber, D. A.; Falk, M.; Schneider, M.; Reich, M.-L.; Sommer, H.; Adelhelm, P.; Janek, J. *Nat. Chem.* **2016**, *8*, 426−434.
(32) Tatsuma, T.; Taguchi, M.; Oyama, N. *Electrochim. Acta* **2001**, *46*, 1201−1205.
(33) Gireaud, L.; Grugeon, S.; Laruelle, S.; Yrieix, B.; Tarascon, J. M. *Electrochem. Commun.* **2006**, *8*, 1639−1649.
(34) Ryou, M.-H.; Lee, D. J.; Lee, J.-N.; Lee, Y. M.; Park, J.-K.; Choi, J. W. *Adv. Energy Mater.* **2012**, *2*, 645−650.
(35) Choi, N. S.; Lee, Y. M.; Park, J. H.; Park, J. K. *J. Power Sources* **2003**, *119−121*, 610−616.
(36) Ding, F.; Xu, W.; Graff, G. L.; Zhang, J.; Sushko, M. L.; Chen, X.; Shao, Y.; Engelhard, M. H.; Nie, Z.; Xiao, J.; Liu, X.; Sushko, P. V.; Liu, J.; Zhang, J.-G. *J. Am. Chem. Soc.* **2013**, *135*, 4450−4456.

DOI: 10.1021/jacs.6b05341
J. Am. Chem. Soc. 2016, 138, 9385−9388